

**Atmospheric pressure single photon laser ionization (APSPLI) mass spectrometry using a 157 nm fluorine excimer laser for sensitive and selective detection of non- to semi-polar hydrocarbons**

5

Christopher P. Rüger<sup>1,2\*#</sup>, Anika Neumann<sup>1,2#</sup>, Martin Sklorz<sup>3</sup>, Ralf Zimmermann<sup>1,2,3</sup>

10

1 Joint Mass Spectrometry Centre, Chair of Analytical Chemistry, University of Rostock,  
18059 Rostock, Germany

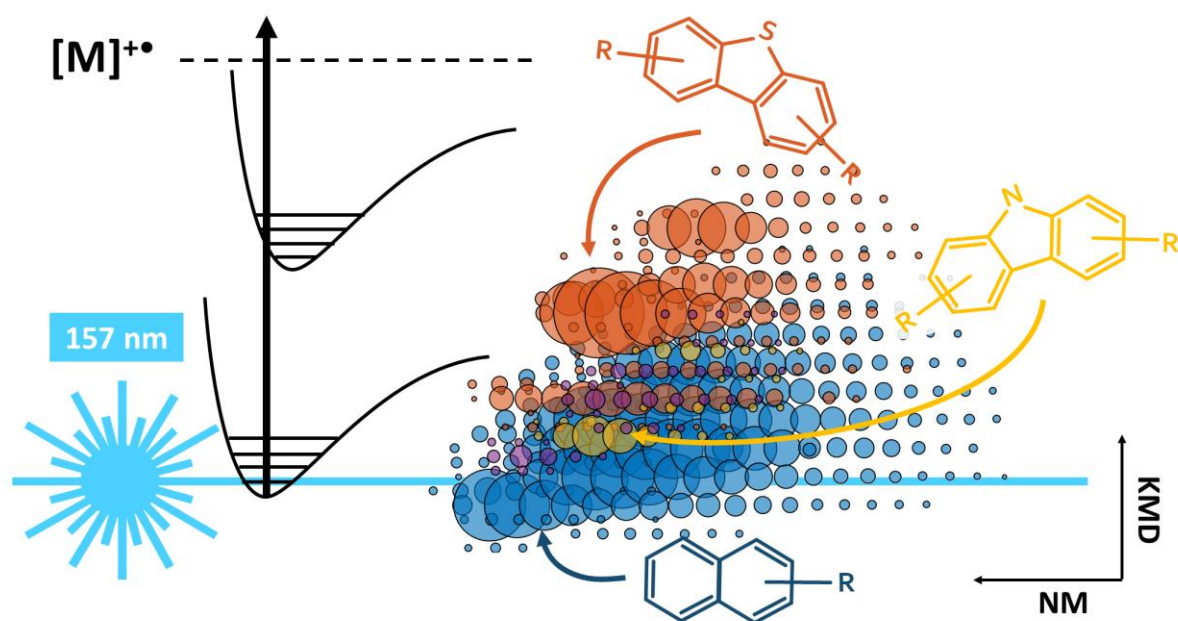
2 Department Life, Light & Matter (LLM), University of Rostock, 18051 Rostock, Germany

3 Joint Mass Spectrometry Centre, Cooperation Group “Comprehensive Molecular Analytics”  
(CMA), Helmholtz Zentrum München (HMGU), 85764 Neuherberg, Germany

15 **Keywords:** atmospheric pressure laser ionization (APLI), excimer laser, high-resolution mass spectrometry, polycyclic aromatic hydrocarbons (PAH), gas chromatography

\* corresponding author, [christopher.rueger@uni-rostock.de](mailto:christopher.rueger@uni-rostock.de)

# these authors contributed equally to the manuscript



## Abstract

In this study, atmospheric pressure single photon ionization (APSPLI) mass spectrometry utilizing a fluorine excimer laser operated at 157 nm (7.9 eV) is presented for the first time. For evaluation and optimization, PAH standard mixtures introduced by gas chromatography were used. Atmospheric pressure laser ionization (APLI) approaches with laser wavelengths above 200 nm induce a multiphoton process, and ionization yields are strongly dependent on the heteroatom-content and isomeric structure. The presented technique using VUV photons allowed for the selective ionization of semi- to non-polar compounds in a single photon ionization process. Consequently, molecular radical cations were found as base peak, whereas protonated species were almost absent. Even though the ionization chamber is flushed by a high flow of pure nitrogen, remaining oxygen and water traces caused several side-reactions, leading to unwanted oxidized ionization artifacts. Installation of a water and oxygen filter cartridge significantly reduced the abundance of those artifacts, whereas the laser beam position was found to have a substantially lower effect. For evaluating complex mixture analysis, APSPLI was applied to characterize a light crude oil subjected to the ionization source by thermogravimetry and gas chromatography hyphenation. In addition to aromatic hydrocarbons, APSPLI also allowed for the sensitive ionization of sulfur-containing aromatic constituents, and even species with two sulfur-atoms could be detected. A comparison of APSPLI to APLI conducted at 266 nm revealed the additional compositional space accessible by the single photon process. This novel ionization concept is envisioned to have a high analytical potential further explored in the future.

## Introduction

With the introduction of electrospray ionization (ESI) in the early 1990s<sup>1,2</sup>, atmospheric pressure ionization (API) techniques have become prevalent in various mass spectrometric research and application fields. In the following two decades, a “zoo” of ionization techniques has been introduced, which can generally be divided into spray, desorption, and discharge concepts<sup>3,4</sup>. Aside from ESI, atmospheric pressure chemical and photoionization (APCI/APPI), direct analysis in real-time (DART), and laser desorption ionization (LDI) are commonly deployed nowadays<sup>3</sup>. The rapid, extensive development of API is primarily driven by two aspects: First, the wide introduction of high-resolution mass spectrometry platforms to analytical laboratories enables the direct infusion of sample material without time-consuming, complex chromatographic pre-separation and motivates the development of selective ionization techniques lowering matrix effects. Second, the analysis of extremely complex sample materials requires the aforementioned selectivity.<sup>5</sup>

High-resolution mass spectrometry has proven to be a powerful approach for the characterization of complex organic mixtures.<sup>5</sup> High-resolution at the  $m/z$ -dimension enables the separation of isobaric species, whereas the high mass accuracy allows for direct chemical conclusions by attributing elemental compositions. The application of selective ionization techniques, chromatographic coupling, or tandem mass spectrometry (MS/MS), further add chemical information.<sup>6–8</sup> In contrast to vacuum ionization techniques, API offers multiple benefits, such as the ease of usage, affordable construction, and collisional-cooling. Nonetheless, atmospheric pressure ionization sources also bear significant analytical drawbacks. They are prone to competing ionization mechanisms and, thus, drastic matrix effects may occur. Moreover, ionization artifacts can commonly be observed, such as clustering, solvent-adducts, and oxidation. Based on the sample preparation and technique, the addition of dopants or sophisticated data processing routines can be required.<sup>9</sup>

Atmospheric pressure photoionization provides low matrix effects and is able to ionize a broad compositional space.<sup>10–13</sup> In classical direct infusion experiments, dopants, such as toluene, are added to enhance the ionization yield.<sup>14,15</sup> Despite infusion approaches solvent-free evolved gas analysis techniques using APPI were reported in literature as well.<sup>16,17</sup> Nonetheless, low sensitivity for certain compound classes or the occurrence of both protonated and radical cations can complicate analysis and interpretation. Consequently, atmospheric pressure laser ionization (APLI) mass spectrometry was developed and first reported by Benter and co-workers in 1999 on a time-of-flight mass spectrometric platform.<sup>18</sup> Laser-based ionization drastically increases the photon density and creates a defined timing and space/geometry for the ionization event. Schiewek et al. introduced evolved gas analysis APLI, in terms of GC-APLI-MS, in 2007 and reported detection limits as low as 5 ng/l for chrysene deploying a resonant ionization by UV laser light at 248 nm.<sup>19</sup> Schrader and co-workers extended this work and

presented detection limits of 2 µg/l for benzonaphthothiophene on an ultrahigh-resolution mass spectrometric system (FT-ICR MS).<sup>20</sup> In the following decade, APLI by 248 nm (KrF-excimer laser)<sup>21</sup> and 266 nm (4<sup>th</sup> harmonic of Nd:YAG solid-state laser) was deployed for the chemical characterization of various petroleum-derived materials, such as crude oil fractions<sup>22–25</sup> and coal<sup>26</sup>, as well as for combustion aerosols<sup>27</sup>, emerging environmental contaminants and pollutants<sup>28–31</sup>, *e.g.*, polycyclic aromatic hydrocarbons (PAHs). Furthermore, the usage of specific dopants or derivatization techniques was studied.<sup>32,33</sup>

Commonly, for vacuum laser ionization, single photon ionization (SPI) and resonance enhanced multi-photon ionization (REMPI) are distinguished.<sup>34,35</sup> Single photon ionization (SPI) realized by VUV-light can be referred to as universal ionization technique, any component with an ionization energy lower than the applied photon energy is ionized, while background gases such as nitrogen or oxygen are not. Resonance-enhanced multi-photon ionization (REMPI) operated at UV-wavelengths exhibit an excited state selectivity and is particularly selective and sensitive towards many aromatic constituents. APLI operated at 266 or 248 nm wavelength is characterized by a two-photon process comparable to the REMPI process, where the absorption of one photon leads to an excited state in the first step and subsequent ionization by absorption of a second photon in the second step generates a radical cation.<sup>33,36</sup> Similar to the REMPI ionization, APLI highlights polycyclic aromatic compounds as well.

In this study, for the best of the author's knowledge, laser ionization mass spectrometry utilizing VUV laser light under atmospheric pressure is reported for the first time. For this purpose, a fluorine excimer laser operating at a wavelength of 157 nm is applied. APLI at 157 nm, corresponding to 7.9 eV, will be able to trigger different ionization pathways compared to the more common APLI approaches. More specifically, it should be able to ionize molecules by absorption of a single photon. Consequently, the concept of APLI at 157 nm is referred to as APSPLI. For REMPI, the lifetime of the excited state of the analytes needs to be long enough allowing the absorption of a second photon, which is prevalently observed for PAHs.<sup>36</sup> Notably, for sulfur-containing polycyclic aromatic hydrocarbons (PASHs) this lifetime is often too short and poor ionization cross-sections are found in APLI.<sup>20</sup> We could show that this behavior is different for APSPLI. Furthermore, shifting the ionization characteristics to predominantly radical cations lowers the spectral complexity, beneficial for the characterization of complex mixtures. In this proof-of-concept study, we introduce APSPLI by analyzing PAH standard mixtures and petroleum-derived highly complex materials. The analytes are subjected to the ionization source by gas chromatographic and thermal analysis hyphenation (evolved gas analysis) avoiding solvent effects. Therefore, ionization characteristics, such as the generation of ionization artifacts and occurrence of radical/protonated species (odd/even electron configuration), can be directly discussed.

## Experimental

### 110 Material

Two different standards of various polycyclic aromatic hydrocarbons, named A4 and M3, were used for evaluation, optimization and validation purpose of the APSPLI setup (Table S1 and Table S2). Briefly, the standard consisted of 14 (A4) and 25 (M3) PAHs, with naphthalene ( $C_{10}H_8$ ,  $m/z$  128.0626) the lightest and coronene ( $C_{24}H_{12}$ ,  $m/z$  300.0939) the heaviest compound, respectively. Concentrations in  
115 the standard ranged between 0.3 to 5 mg/L. The applicability of APSPLI for the description of complex organic mixtures was evaluated with petroleum-derived material. For this purpose, a light crude oil (CPC Blend from Kazakhstan, Gunvor Raffinerie Ingolstadt GmbH) was chosen. This specific crude oil sample was already investigated by comprehensive gas chromatography time-of-flight mass spectrometry in the literature.<sup>37</sup>

### 120 Method

All analyses were carried out on a Bruker Apex II ultra Fourier transform ion cyclotron resonance mass spectrometer (Bruker Daltonics, Bremen, Germany) equipped with a 7 Tesla superconducting magnet. A commercial GC-APCI II source (Bruker Daltonics, Bremen, Germany) was modified for atmospheric pressure laser ionization operation. This modification was realized by exchanging the glass viewports  
125 at the left- and right-hand side ( $90^\circ$ , rectangular to the sample inlet and mass spectrometric inlet) with magnesium fluoride windows ( $MgF_2$ -VUV-window, laser polished,  $25 \pm 0.2$  mm diameter,  $2 \pm 0.1$  mm depth, Korth Kristalle GmbH, Altenholz, Kiel). A photographic and schematic representation of the system can be found in Figure 1. For ionization, the 157 nm radiation emitted by a fluorine excimer laser (Compex Pro F2, Lamda Physik AG, Göttingen, Germany) daily refilled with fluorine gas ( $4.99 \pm 0.15$   
130 v-% fluorine in helium, Air Liquide, Hamburg, Germany) was used with a beam diameter of 7 mm clipped by a cylindrical aperture. A laser repetition rate of 10 Hz was used for all experiments. Laser power was between 25 and 43 mW (20 ns pulse width, pulse energy 2.5 – 4.3 mJ) measured after the transmission through the ion source by a VUV laser sensor (PEM 24K VUV, Laser Optics Scientific Instruments, RBM R. Braumann GmbH, Langenbach, Germany). At the mass spectrometer's entrance,  
135 a flat spray shield was mounted on the glass capillary used for ion transmission from atmospheric pressure to the first vacuum stage at 3.5 mbar. The concentration of remaining oxygen and water inside the ionization chamber was reduced by installing a water (Gas Clean GC/MS Filter, CP17973, Varian Technologies, Palo Alto, CA, USA) and oxygen filter cartridge (SGT Oxygen Filter, Scientific Glass Technology, Sgt Middelburg B.V., Middelburg, Netherlands) within the development and optimization  
140 process.

The beamline between laser exit and ion source window is realized by plastic tubing sealed on both sides with common vacuum flange connectors and O-ring sealings. The beamline is flushed with several liters per minute of dry nitrogen (purity > 99.999 %) to prevent significant attenuation of the laser beam due to absorption of the VUV photons by oxygen or moisture.

145 Gas chromatographic analyses were performed on a CP 3800 system (Agilent, former Varian Technologies, Palo Alto, CA, USA) equipped with a programmable temperature vaporizer (PTV) injector. A 5%-phenylmethylsilicone column (Restek, Bad Homburg, Germany) with a length of 30 m, 320  $\mu\text{m}$  inner diameter and 0.1  $\mu\text{m}$  film thickness was used for separation. Helium (99.999 v-% purity) was used as carrier gas with a constant head pressure of 2.1 (Method 1) and 0.7 bar (Method 2). The  
150 temperature ramp of the GC oven was as following: Method 1 – hold for 3 min at 30 °C, raise to 300 °C with 5 K/min and hold 5 min, Method 2 – hold for 3 min at 30 °C, raise to 320 °C with 5 K/min and hold 2 min. The PTV injector equipped with a straight inlet liner was kept 1 min at 65 °C and then raised with 100 K/min to 300 °C held for 5 min. For thermal analysis, a TG 209 thermobalance (Netzsch Gerätebau GmbH, Selb, Germany) was used. The samples were heated from 20 to 600 °C in an  
155 aluminum crucible under nitrogen atmosphere (99.999 v-% purity) after 2 min initialization at 20 °C with a heating rate of 10 K/min. Further details on the gas chromatographic<sup>38,9</sup> and thermogravimetric<sup>17,39</sup> hyphenation to the atmospheric pressure ionization source of the ultrahigh resolution mass spectrometer can be found elsewhere. For both cases, the transferline was kept at 280 °C.

160 One  $\mu\text{L}$  of the PAH standard mixtures was injected for GC analysis. The light crude oil (CPC blend) was diluted by a factor 1000 (1000 v-ppm) in dichloromethane and 1  $\mu\text{L}$  of the diluted sample was injected into the PTV injector for GC analysis. For thermogravimetric analysis, 1-5 mg of the sample material was directly placed in the aluminum crucible.

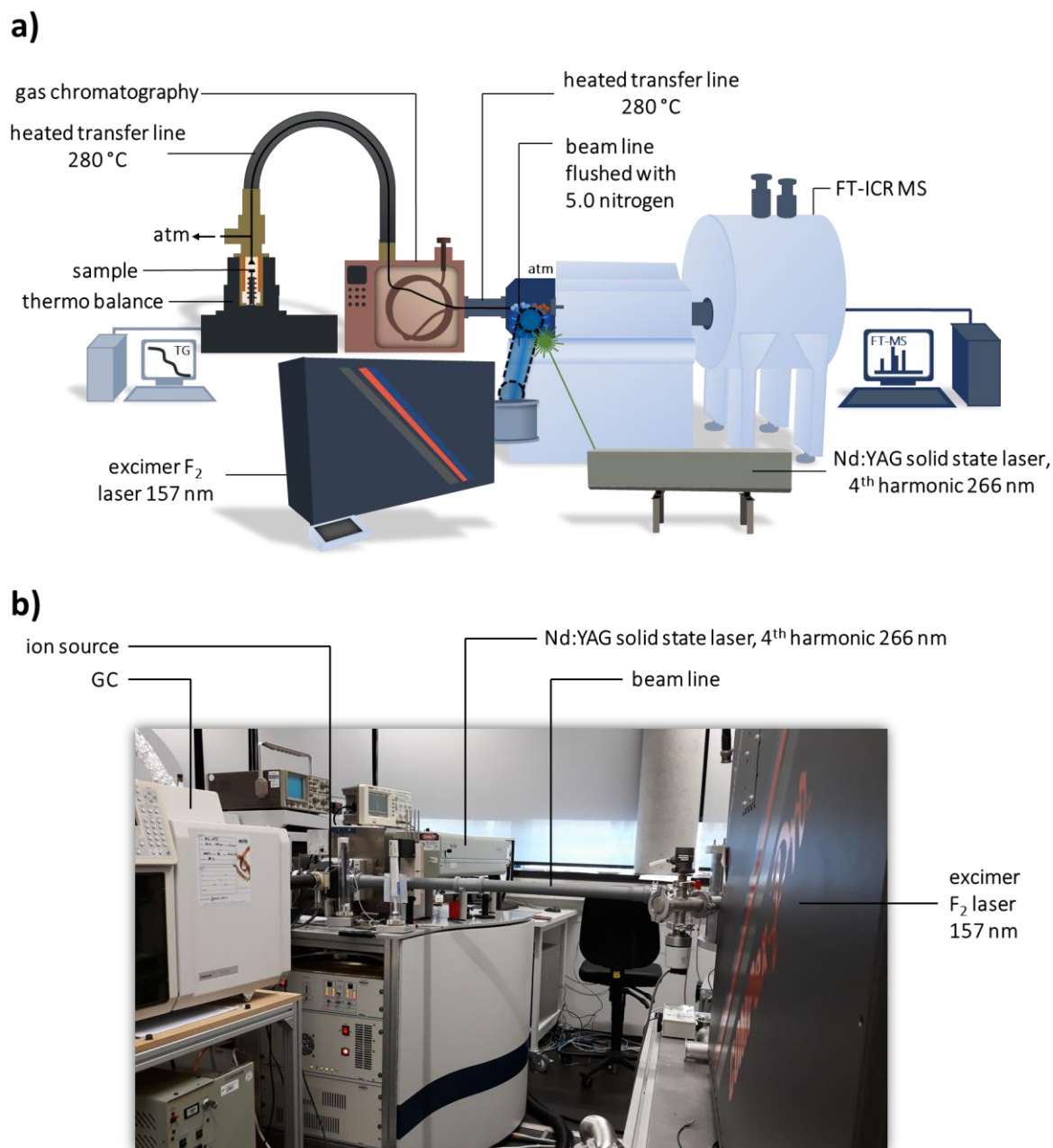
The mass spectrometer was operated in positive ion mode. The nebulizer gas flow rate was varied  
165 between 1.5 to 6 l/min and the dry gas flow was set to 3 l/min with a temperature of 220 °C. Mass spectra were recorded from  $m/z$  100 to 1,000 with a transient length of approximately 2 s (4 megawords), resulting in a resolving power of roughly 260,000 at  $m/z$  400.

## Data analysis

Data processing was divided into two main steps. General evaluation and  $m/z$ -calibration of the mass  
170 spectrometric data was carried out in Bruker Data Analysis 5.0 (Bruker Daltonics, Bremen, Germany). Internal  $m/z$ -calibration of the petroleum-derived sample materials was performed using a list of alkylated PAH and PASH species covering the complete mass range. After peak picking ( $\geq S/N$  9), the data were exported by self-written Visual basic scripts.<sup>38,39,9</sup>

175 Subsequently, the exported data were processed by a self-written MATLAB-based (MATLAB R2019b) graphical user interface named CERES (Computing enhanced resolution spectra). An error of 2 ppm for elemental composition attribution was applied. The following elemental composition boundaries were deployed:  $C_{6-100}H_{6-100}N_{0-2}O_{0-5}S_{0-2}$ . Root-mean-square-errors (RMSE) of the final assignments after further attribution rules below 0.5 ppm were found.





180 **Figure 1:** a) Scheme of the atmospheric pressure single photon laser ionization (APSPLI) setup using a fluorine excimer laser with an emission wavelength of 157 nm. The Nd:YAG solid state laser operated at the 4<sup>th</sup> harmonic (266 nm) for APLI is also depicted. b) Photographic image of the laser ionization system coupled to the ultrahigh resolution mass spectrometer (FT-ICR MS).

## Results and Discussion

### 185 *Polycyclic aromatic hydrocarbon standard*

In the first part of the study, the general mass spectrometric response of the newly developed ionization approach will be discussed. Evaluation and optimization of utilizing the fluorine excimer laser (157 nm) for single photon ionization at atmospheric pressure were done by subjecting PAHs by gas chromatographic separation to the ionization chamber. Figure 2 shows the observed total ion chromatogram (TIC). Except for naphthalene, biphenyl, and acenaphthylene, all PAHs from the standard mixtures could be detected, with the radical cation (odd electron configuration) being the most prominent signal. Naphthalene, acenaphthylene, biphenyl, and methyl eicosanoate were not observed due to their higher ionization energies of 8.12 – 8.15, 8.12, 8.16 eV, and > 10 eV compared to the VUV photon energy of the excimer laser of 7.9 eV.<sup>40,41</sup> These findings indicate that the ionization process is solely realized by direct single photon ionization and not by multiphoton ionization or chemical reaction cascades.

Without further adaption of the commercial atmospheric pressure ionization source, detection limits in the sub-ppb level can be estimated for the gas chromatography coupling. This high sensitivity is suggested to result from the very high photon density in the laser beam compared to the divergent light of classical krypton discharge lamps deployed for APPI. For species below a double bond equivalent (DBE) of 10 (3-ring PAHs), the sensitivity drastically increases with increasing aromaticity. A slight trend of increased sensitivity can be observed for the PAHs with three to seven conjugated aromatic rings. Nonetheless, for those analytes, the overall normalized response was within one order of magnitude. In classical REMPI, the ionization cross-section and, thus, mass spectrometric response varies drastically with the isomeric structure, *e.g.*, at 266 nm phenanthrene is considerably better ionized than anthracene.<sup>42,36</sup> For the presented APSPLI approach the behavior is more comparable to vacuum single photoionization, where ionization cross-sections were reported to vary within one order of magnitude.<sup>43–45</sup>

As noticeable from the TIC in Figure 2, APSPLI provides a very low and nearly absent chemical background noise as a clear advantage. Other gas-phase atmospheric pressure ionization techniques can cause substantial chemical background noise, *e.g.*, APCI efficiently ionizes siloxanes released from the column at higher temperatures. Chemical noise complicates data interpretation and could cause matrix effects or ionization suppression.<sup>38,9</sup> This valuable behavior of APSPLI is caused by the selective ionization process for compounds having an ionization potential low enough for single photon ionization by the 157 nm radiation.

Interestingly, PAHs can also be found as doubly charged ( $z=2$ ) species with relative abundances from below the detection limit up to 5 % of the singly charged molecular ion abundance. In particular, for larger aromatic species, such as indeno[1,2,3,c,d]pyrene ( $C_{22}H_{12}$ ,  $m/z$  276, DBE 17) (Figure S1), this effect can be observed.

220 Comparable to APPI conducted with a krypton discharge lamp (124/117 nm emission), oxygen is a critical parameter when using VUV-light for ionization under atmospheric pressure conditions. Oxygen and moisture in the ionization chamber substantial impact the ionization characteristics leading to an unwanted formation of oxidized ionization artifact. The formation of those artifacts is a drawback of APSPLI. By absorbing a VUV photon, oxygen or water molecules are photolyzed into oxygen or hydroxyl  
225 radicals. Oxygen radicals may subsequently recombine with intact oxygen molecules forming highly reactive ozone ( $O_3$ ).<sup>46</sup> Ozone readily reacts with organic constituents creating oxidized products. Nonetheless, the occurrence of oxidized species as an ionization artifact was also reported for atmospheric pressure chemical ionization.<sup>9</sup> In the first optimization step, this influence can be minimized by careful flushing and heating the ionization chamber for several hours prior usage.

230 Pyrene is reported to be particularly susceptible to this kind of oxidation reaction.<sup>47,48</sup> The concentration of oxygen in the ionization chamber atmosphere is crucial for this process. Figure 3 a and b display this effect by comparing the APSPLI spectra for an oxygen concentration of approximately 200 ppm and 10 ppm. In this example, pyrene was introduced into the APSPLI source by thermogravimetric hyphenation at a constant concentration of approximately 300 ppb. High oxygen  
235 levels (Figure 3 a) will cause oxidation of the analyte and the mono-oxidized radical cation ( $C_{16}H_{10}O^{+}$ ) was found to be as intense as the molecular ion ( $C_{16}H_{10}^{+}$ ). Even a series of multiple oxidized species, up to  $C_{16}H_{10}O_3^{+}$ , and the respective protonated species could be detected. This intense reaction cascade increases the spectral complexity drastically and hinders chemical interpretation and complex mixture analysis. Nonetheless, a reduction of the oxygen concentration by a factor of approximately  
240 20 to the low ppm-level (Figure 3 b) completely changes this picture and will lead to a drastic reduction of ionization artifacts. The molecular ion is the base peak, and the mono-oxidized species was found with an abundance of around 10 %. Other ionization artifacts were below the detection limit or almost absent. Moreover, Figure 3 c shows the effect after deploying a software filter in the mass spectrometric processing using the automated elemental composition attribution and removing the  
245 signals attributed to the  $CHO_x$ -class.

The nebulizer gas flow itself influences the intensity of the abundance of the radical cation to a slight extent, with largest values for 1.5 l/min and lowest for the highest setting of 6.0 l/min. The abundance of the protonated species remains unaffected. Beneficially, oxidation is lowest for the highest nebulizer gas flow due to a decrease in ionization chamber gas exchange time. However, the highest nebulizer

gas flow showed the lowest absolute signal intensities, whereas, for the lowest flow rate, the highest signal abundance can be observed. Therefore, adapting the nebulizer gas flow for lowering ionization artifacts is not suggested as a favorable option. The comparable low-flow setting (1.5 l/min) giving the highest signal abundances was chosen.

Oxygen concentration and moisture of the nebulizer and purge gas have a high impact, as shown in Figure 3 for pyrene. Consequently, the water and oxygen level in the ionization source was reduced by the installation of water and oxygen filter cartridges for the nebulizer nitrogen gas supply. A reduction of the abundance of oxidized ionization artifacts by a factor of two to four was achieved for the PAHs covering three- to seven-ring aromatic structures (Figure S2). The reduction was especially efficient for 3-4-ring aromatic species, such as anthracene, fluoranthene, and pyrene. The presence of multiply oxidized ionization artifacts was reduced largely, and those species are entirely absent for most of the analytes. It can be found that installing either the water or oxygen filter slightly reduces the oxidation artifacts, but the combination of both filter cartridges gave the best results and was used for all further investigations. It has to be noticed that the filter cartridges have limited capacity and need to be replaced or reconditioned frequently. The application of both filter cartridges resulted in ionization artifacts of approximately 10 % for most of the analytes. Some PAHs are very prone to oxidation, such as acenaphthene, for which the abundance of the oxidized species could only be reduced to approximately 35 % of the molecular radical cation.

Laser ionization techniques allow controlling the timing and the position of the ionization event. Hence, the influence of the laser beam position on the signal intensity and ionization characteristics was investigated. Three different positions for the laser beam were investigated (Figure S3): 1) beam position near the GC effluent capillary, 2) beam position in the middle between GC effluent and mass spectrometry inlet, and 3) beam position in front of the mass spectrometry inlet. The highest intensities for the molecular radical cations of the respective standard compounds were found for 1) and 2), whereas the abundance is up to five-times lower for ionization close to the mass spectrometry inlet (Figure S4). These findings can be explained by the flow conditions in the ionization chamber. Analytes subjected to the source are diluted in the source volume and, thus, concentration of the neutral molecules is highest at the sample inlet and lowest at the mass spectrometry inlet. Keeping the laser beam geometry and size constant, a reduced number of molecules are struck by the VUV photons with increasing distance to the sample inlet. More interestingly, the variation in proportion of oxidized species is not as pronounced. A slightly higher contribution of the oxygenation artifact was found for the centered position for all analytes, except anthracene. Position 1) and 3) revealed comparable strengths of oxidation. Interestingly, the position of the laser beam does not influence the ionization behavior regarding the partitioning between radical cations (odd-type) and protonated

species (even-type) significantly. Summarizing, positioning the laser beam close to the sample inlet  
285 was found to be the optimized location.

The optimization process allowed ionization artifacts to be reduced significantly. We want to emphasize the value of APSPLI, particularly for chromatographic hyphenation or high-resolution mass spectrometry. Here, ionization artifacts can be further removed from the data set by intelligent processing algorithms tracing the time-resolved chemical signatures of the molecular ion and  
290 corresponding oxidized species.<sup>38,9</sup> With this approach, a non-targeted investigation of complex organic mixtures containing oxygenated species is feasible. Species not containing oxygen, such as CH-, CHS-, and CHN-class compounds, can be sensitively characterized by deploying the software filter shown in Figure 3 c.

#### *Complex mixture analysis*

295 Evaluation of the APSPLI approach for the chemical description of complex organic mixtures was performed on a light crude oil (CPC Blend). The crude oil was subjected to APSPLI by gas chromatography and thermal analysis.<sup>39,9</sup> Although the separation power of thermal analysis is much lower compared to gas chromatographic hyphenation, almost the same compositional space, *i.e.*, compound classes, mass range, and isobaric complexity, could be detected. Gas chromatographic  
300 hyphenation generally leads to lower matrix effects for atmospheric pressure ionization techniques. However, finding the same compositional space for GC and TG coupling indicates relatively low matrix effects for APSPLI. Figure 4 a) shows the survey diagram, with insets of the total ion chromatogram (TIC) and base peak chromatogram (BPC). A characteristic and complex desorption pattern of the petroleum-derived material can be found.

305 Attribution of the elemental compositions to the molecular pattern ionized by APSPLI revealed the CH-class as the most dominant compound class. Nonetheless, also CHS<sub>1</sub>-, CHO<sub>1</sub>-, CHN<sub>1</sub> and CHS<sub>1</sub>O<sub>1</sub>-class constituents were detected with considerable abundance. All classes revealed a homologous alkylation pattern (Figure 4 c). The Kendrick plot<sup>49</sup>, normalized to the alkylation-pattern (CH<sub>2</sub>), given in Figure 4 b, further points out the molecular diversity and the covered compositional space. The alkylation pattern  
310 of the CH-class covered a DBE range of 5 (*e.g.*, indane-derivatives) up to 19 (*e.g.*, coronene-derivatives) with the DBE series of 9 (*e.g.*, acenaphthylene-derivatives) at highest abundances. Predominantly, radical cations were detected (Figure S5) and protonated were found species below 1 % of the total ion count. This beneficial characteristic of APSPLI allows simplifying the immense isobaric complexity, and for the given high complex petroleum-derived material, 5-10 signals per nominal mass could be  
315 detected (Figure 4 d). In contrast, APPI commonly generates both electron configurations (odd/even-type) to the same extent, which would yield > 15-20 signals per nominal mass.

For the PAH standard mixture measurements, oxidation was found as a considerable ionization artifact. For the light crude oil, however, the abundance of the CHO-class was found to be below 4 %. Furthermore, the DBE distribution of the CH-class was found to be Gaussian-shaped, whereas the CHO-class revealed an entirely different non-uniform pattern. (Figure S4). The same can be found comparing the CHSO- and CHS-class DBE distributions. Presuming a considerable effect of oxidation would lead to a comparable pattern. This discrepancy suggests that only a minor percentage of the CHSO- and CHO-class might result from oxidation in the ionization source. Moreover, detection of the artifacts based on the gas chromatographic separation is feasible.<sup>9</sup> This approach detected artificial in-source oxidation only to a low extent and further strengthens the finding that we were able to ionize and detect oxygen-containing species as constituents of the petroleum-derived material.

Sulfur-containing aromatic and polyaromatic hydrocarbons (PASH), such as thiophenes and benzothiophenes, are generally poorly detected by REMPI/APLI. This effect is due to the short lifetime of the excited state leading to low ionization cross-sections. The same effect can be found for certain oxygenated and halogenated PAHs. For VUV photoionization at atmospheric pressure (APPI) with shorter wavelength (*e.g.*, 117 and 124 nm), those compound classes are primarily detected as a mixture of odd and even species due to complex reaction cascades, but generally with good sensitivities. Accordingly, the presented APSPLI approach allowed the ionization and mass spectrometric detection of PASHs as well. Interestingly, those species are ionized very efficiently, being the second most abundant compound class. In the average mass spectrometric response (Figure 4 c) a series of CHS<sub>1</sub>-constituents with a DBE of 9 (tentatively dibenzo- and naphthothiophenes) can be found as high abundant homologous alkylation series with C<sub>16</sub>H<sub>16</sub>S<sub>1</sub> as base peak. Comprehensive gas chromatographic analysis (GCxGC) of the same light crude oil revealed semi-quantitatively dibenzothiophenes (~1 %) and benzothiophenes (< 1 %) as sulfur-containing constituents.<sup>37</sup> For APSPLI, benzonaphthothiophenes (CHS<sub>1</sub>-class, DBE 12), hardly detected at all with the GCxGC, were detected as the second most dominant aromatic core structure for the CHS<sub>1</sub>-class. Interestingly, even CHS<sub>2</sub>-class species were detected with APSPLI (Figure 4 d) but not detected by GCxGC.

APLI conducted at wavelengths above 200 nm, in the following referred to as APMPLI, ionizes PAHs with high sensitivity and selectivity. This feature helps to reduce matrix effects and allows for targeted analysis. However, also a certain part of the compositional space of a complex mixture might be missed. Figure 5 compares the compositional space ionized by APSPLI and APMPLI (266 nm). APMPLI is able to ionize aromatic CH-class compounds more efficiently compared to APSPLI. Moreover, the pattern is also different and APMPLI addresses high aromatic species more efficiently. This finding can be explained by the strong variation of ionization cross-section of several order of magnitudes for the REMPI process in APMPLI. Due to this behavior, quantification aspects are hardly feasible, and certain classes are not detected at all. In contrast, APSPLI broadens the compositional space and aside of the

sulfur-containing species discussed above, nitrogen-containing constituents can be found. In comparison, carbazoles (CHN<sub>1</sub>-class) were only found with 0.01 % abundance for the GCxGC measurements.<sup>37</sup>

355 The Kendrick mass defect plot (Figure 5) emphasizes the additional information of APSPLI by giving access to further compound classes. APSPLI is able to address complex mixtures and a broadened chemical space of semi- to non-polar constituents could be detected. Particularly, hetero-atom containing compounds, such as the CHN- and CHS-class, were detected with good ionization yield beneficially compared to classical APLI.

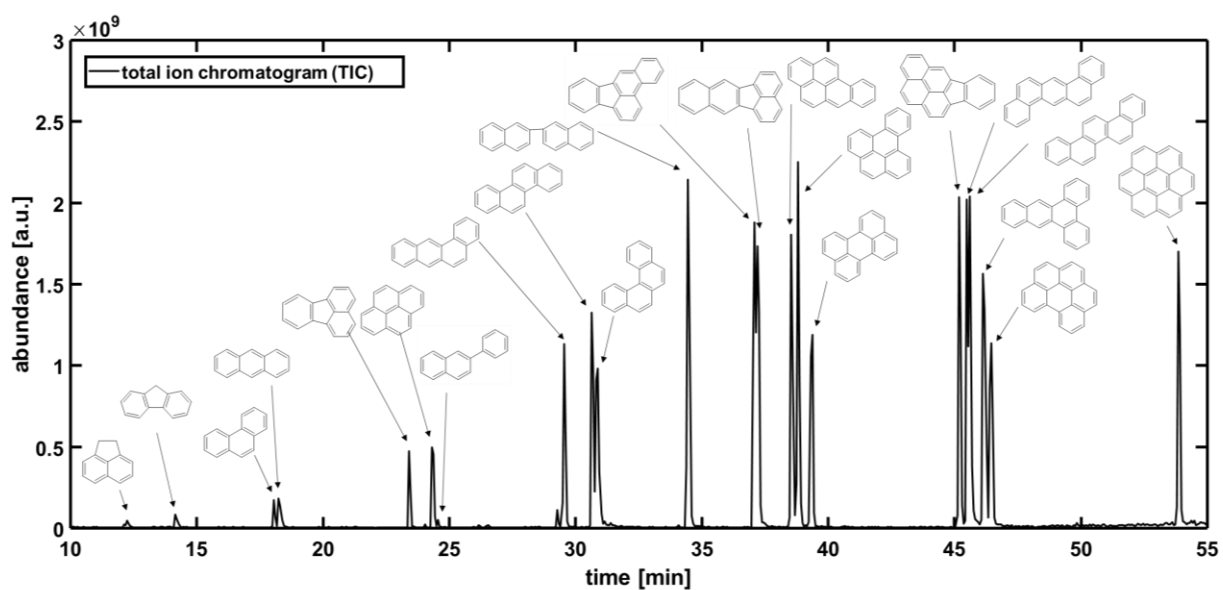


**Figure 2:** Gas chromatographic separation of the M3 PAH standard mixture ionized by atmospheric pressure single photon ionization with 157 nm. All constituents, except naphthalene, biphenyl, acenaphthylene, and methyl eicosanoate, could be detected. The reason is that for the latter compounds, the ionization energies are larger than 7.9 eV. Signal to noise levels for the PAHs introduced at low ppm level were between several hundred and above ten thousand.



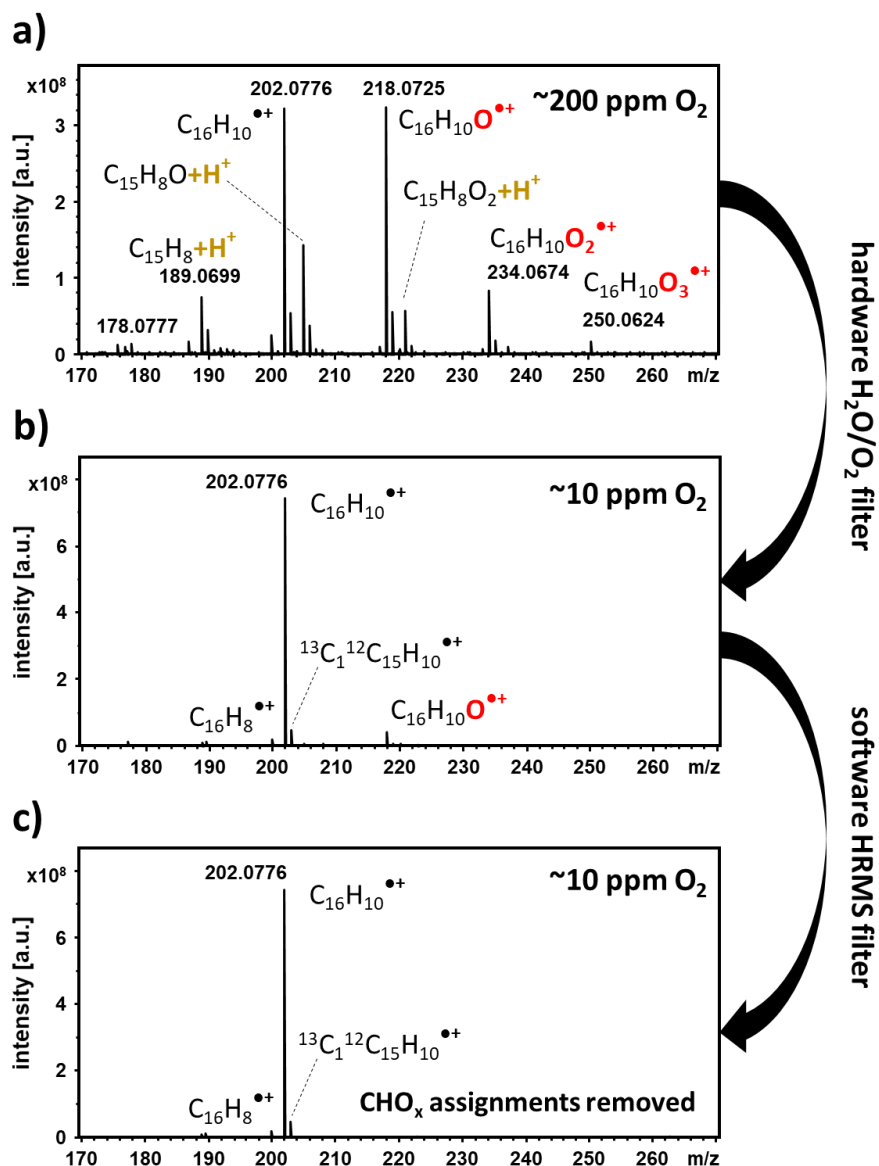


**Figure 3:** Pyrene ( $C_{16}H_{10}$ ,  $m/z$  202) subjected to 157 nm APSPLI by thermogravimetry coupling keeping the crucible at constant 90 °C. The mass spectrometric pattern of the molecular ion (radical ions, odd-electron configuration), quasi-molecular ion (protonated species, even-electron configuration), and oxidized artifacts is depicted. a) at 200 v-ppm, b) at 10 v-ppm oxygen (after installation of an oxygen- and water-filter, and c) after installation of the hardware filter and deploying a software filter in the mass spectrometric processing removing the signals attributed to the  $CHO_x$ -class.

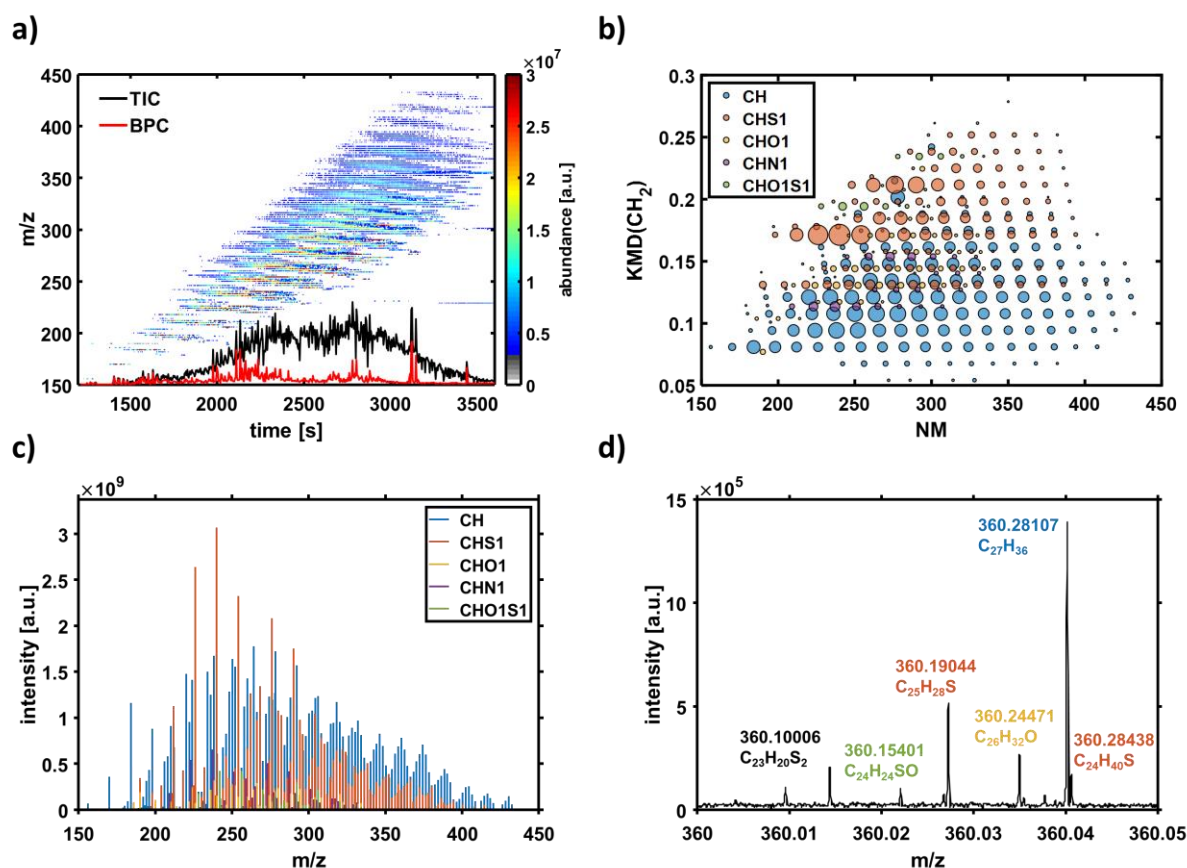
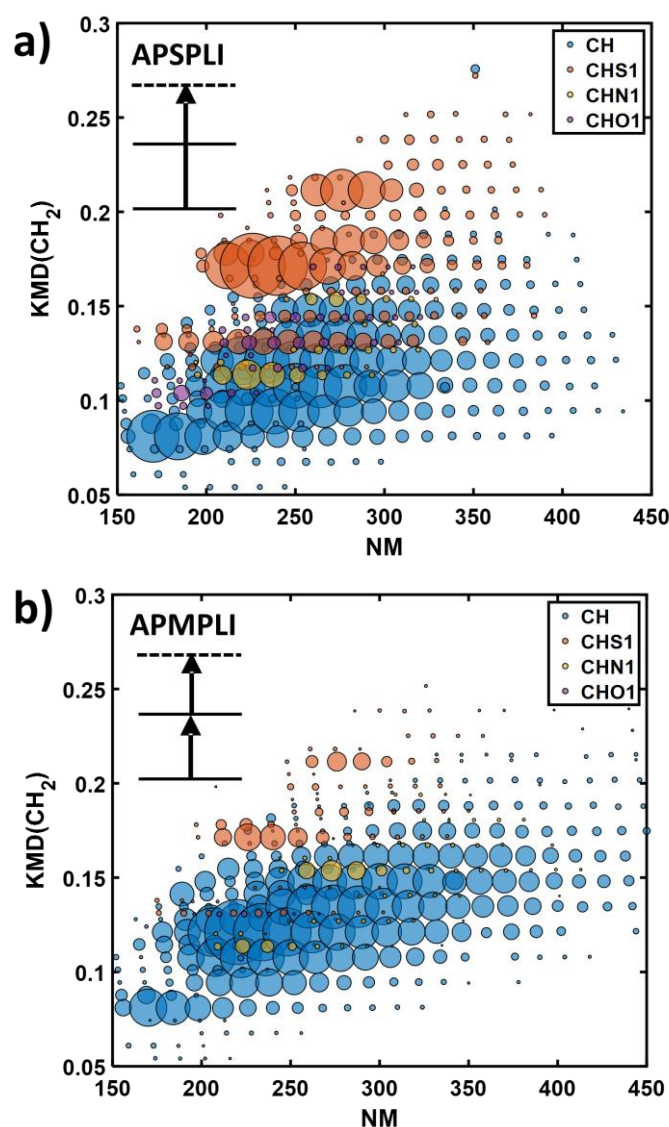


**Figure 4:** Gas chromatography atmospheric pressure single photon laser ionization (APSPLI, 157 nm) of a light crude oil (CPC Blend, Kazakhstan). a) Survey diagram (time versus  $m/z$ ) with total ion count (TIC) and base peak chromatogram (BPC) as inset, b)  $CH_2$ -based Kendrick mass defect plot color-coded according to the attributed compound class and size coded according to the summed abundance, c) average mass spectrum color-coded according to the attributed compound class, and d) mass spectrometric enlargement to the nominal mass 360 with attributed elemental compositions.



380

**Figure 5:** CH<sub>2</sub>-based Kendrick mass defect (KMD) diagram of a light crude oil (CPC Blend, Kazakhstan) subjected to the ionization source by thermal analysis coupled to-FT-ICR MS: a) Deploying APSPLI (157 nm) and b) atmospheric pressure multiphoton laser ionization (APMPLI, 266 nm). The nominal mass (NM) is depicted at the abscissa. Elemental composition attribution is color-coded according to the attributed compound class and size coded according to the summed abundance. The detectability of sulfur species by APSPLI becomes clear. This renders APSPLI to be particularly interesting for analyses of (heavy) petrochemical matrices.

385

## Conclusion

In this proof-of-concept study, we could present the first application of laser-based VUV-radiation for the ionization at atmospheric pressure (APSPLI) in high-resolution mass spectrometry. For this purpose, a fluorine excimer laser operating at 157 nm was installed at an FT-ICR MS.

Based on the evaluation with PAH standard mixtures, we could show the selective ionization of constituents with an ionization potential below the photon energy of 7.9 eV. Consequently, constituents, such as naphthalene, biphenyl, and acenaphthylene, were not detected. An ionization process driven by single photon ionization is clearly proven. APSPLI dominantly produces molecular radical cations with high sensitivity and low abundance of protonated species. This feature significantly reduces the spectral complexity. Nonetheless, residual oxygen and water in the ion source atmosphere were found to be crucial parameters, and side-reactions caused the unwanted generation of oxidized ionization artifacts. However, those artifacts could be reduced by applying water and oxygen filter cartridges to further purify the nitrogen supply, high nitrogen flow rates, and the ionization of the analytes nearby the inlet of the ionization chamber.

APSPLI could successfully be applied for the characterization of a complex organic mixture (light crude oil). CH-class constituents were found as the dominant compound class. APSPLI allowed for a sensitive ionization of sulfur-containing aromatic constituents and even CHS<sub>2</sub>-class species could be detected. Moreover, CHN-class compounds were found with increased abundance compared to APLI. Hence, APSPLI was found to be able to ionize a broad compositional space. Due to the single photon ionization process, APSPLI is able to overcome the limitations of classical APLI.

Future studies will focus on the optimization of ionization conditions and improved ionization geometry with the motivation for a drastic reduction of side-reactions. The high sensitivity may help in the characterization of low concentrated ultra-complex mixtures, such as emerging pollutants or carbonaceous aerosol emissions. Furthermore, APSPLI may address chlorine- or bromine-containing analytes, which are difficult to ionize by multiphoton processed due to high intersystem crossing rates, as well as unstable compounds such as organometallic complexes. From an instrumental perspective, the compositional space accessed by APSPLI will be further broadened by deploying laser technologies with even shorter wavelengths, such as 118 nm from non-linear frequency conversion of Nd:YAG lasers or the 116 nm and 123 nm lines of the hydrogen laser.

## Acknowledgment

Funding by the Horizon 2020 program for the EU FT-ICR MS project (European Network of Fourier-Transform Ion-Cyclotron-Resonance Mass Spectrometry Centers, Grant agreement ID: 731077) is gratefully acknowledged. The authors thank the German Research Foundation (DFG) for funding of the Bruker FT-ICR MS (INST 264/56).

## Supplemental Material

The Supporting Information is available free of charge at

Table S1 and Table S2 list the composition and concentration of the PAH standard mixtures. Figure S1 exhibits APSPLI mass spectrum of indeno[1,2,3,c,d]pyrene. Figure S2 shows the effect of deploying an oxygen-, a water-filter, and both filter types for purification of the nebulizer gas supply. Figure S3 gives a scheme of the laser beam position ionization. Figure S4 reveals the effect of the different ionization positions on the radical cation abundance. Figure S5 displays the compound class distribution of the light crude oil ionized by APSPLI. Figure S6 depicts the double bond equivalent pattern of various compound classes ionized by APSPLI.

## References

- (1) Fenn, J. B.; Mann, M.; Meng, C. K.; Wong, S. F.; Whitehouse, C. M. *Science (New York, N.Y.)* **1989**, DOI: 10.1126/science.2675315.
- 435 (2) Fenn, J. B.; Mann, M.; Meng, C. K.; Wong, S. F.; Whitehouse, C. M. *Mass Spectrom. Rev.* **1990**, DOI: 10.1002/mas.1280090103.
- (3) Alberici, R. M.; Simas, R. C.; Sanvido, G. B.; Romão, W.; Lalli, P. M.; Benassi, M.; Cunha, I. B. S.; Eberlin, M. N. *Analytical and bioanalytical chemistry* **2010**, DOI: 10.1007/s00216-010-3808-3.
- (4) Venter, A.; Nefliu, M.; Graham Cooks, R. *TrAC Trends in Analytical Chemistry* **2008**, DOI: 10.1016/j.trac.2008.01.010.
- 440 (5) Schmitt-Kopplin, P.; Kanawati, B. *Fundamentals and Applications of Fourier Transform Mass Spectrometry*; Elsevier: San Diego, 2019.
- (6) Kondyli, A.; Schrader, W. *Journal of mass spectrometry : JMS* **2019**, DOI: 10.1002/jms.4306.
- (7) Li, D.-X.; Gan, L.; Bronja, A.; Schmitz, O. J. *Analytica chimica acta* **2015**, DOI: 10.1016/j.aca.2015.08.002.
- 445 (8) Panda, S. K.; Andersson, J. T.; Schrader, W. *Angewandte Chemie (International ed. in English)* **2009**, DOI: 10.1002/anie.200803403.
- (9) Schwemer, T.; Rüger, C. P.; Sklorz, M.; Zimmermann, R. *Analytical chemistry* **2015**, DOI: 10.1021/acs.analchem.5b02114.
- (10) Hanold, K. A.; Fischer, S. M.; Cormia, P. H.; Miller, C. E.; Syage, J. A. *Analytical chemistry* **2004**, DOI: 10.1021/ac035442i.
- 450 (11) Huba, A. K.; Huba, K.; Gardinali, P. R. *The Science of the total environment* **2016**, DOI: 10.1016/j.scitotenv.2016.06.044.
- (12) Rogel, E.; Witt, M. *Energy Fuels* **2017**, DOI: 10.1021/acs.energyfuels.6b02363.
- (13) Witt, M.; Timm, W. *Energy Fuels* **2016**, DOI: 10.1021/acs.energyfuels.5b02353.
- 455 (14) Kauppila, T. J.; Kersten, H.; Benter, T. *Journal of the American Society for Mass Spectrometry* **2014**, DOI: 10.1007/s13361-014-0988-7.
- (15) Kauppila, T. J.; Kuuranne, T.; Meurer, E. C.; Eberlin, M. N.; Kotiaho, T.; Kostianen, R. *Analytical chemistry* **2002**, DOI: 10.1021/ac025659x.
- (16) Kostyukevich, Y.; Zhrebek, A.; Vlaskin, M. S.; Borisova, L.; Nikolaev, E. *Analytical chemistry* **2018**, DOI: 10.1021/acs.analchem.8b02043.
- 460 (17) Rüger, C. P.; Grimmer, C.; Sklorz, M.; Neumann, A.; Streibel, T.; Zimmermann, R. *Energy Fuels* **2018**, DOI: 10.1021/acs.energyfuels.7b02762.
- (18) Schmidt, S.; Appel, M. F.; Garnica, R. M.; Schindler, R. N.; Benter, T. *Analytical chemistry* **1999**, DOI: 10.1021/ac9901900.
- 465 (19) Schiewek, R.; Schellenträger, M.; Mönnikes, R.; Lorenz, M.; Giese, R.; Brockmann, K. J.; Gäb, S.; Benter, T.; Schmitz, O. J. *Analytical chemistry* **2007**, DOI: 10.1021/ac0700631.
- (20) Schrader, W.; Panda, S. K.; Brockmann, K. J.; Benter, T. *The Analyst* **2008**, DOI: 10.1039/b801031e.
- (21) Kersten, H.; Lorenz, M.; Brockmann, K. J.; Benter, T. *Journal of the American Society for Mass Spectrometry* **2011**, DOI: 10.1007/s13361-011-0112-1.
- 470 (22) Benigni, P.; DeBord, J. D.; Thompson, C. J.; Gardinali, P.; Fernandez-Lima, F. *Energy Fuels* **2016**, DOI: 10.1021/acs.energyfuels.5b02292.
- (23) Gaspar, A.; Zellermann, E.; Lababidi, S.; Reece, J.; Schrader, W. *Energy Fuels* **2012**, DOI: 10.1021/ef3001407.
- 475 (24) Gaspar, A.; Zellermann, E.; Lababidi, S.; Reece, J.; Schrader, W. *Analytical chemistry* **2012**, DOI: 10.1021/ac300133p.
- (25) Lababidi, S.; Schrader, W. *Rapid communications in mass spectrometry : RCM* **2014**, DOI: 10.1002/rcm.6907.

- 480 (26) Meyer, W.; Seiler, T.-B.; Schwarzbauer, J.; Püttmann, W.; Hollert, H.; Achten, C. *The Science of the total environment* **2014**, DOI: 10.1016/j.scitotenv.2014.06.140.
- (27) Stader, C.; Beer, F. T.; Achten, C. *Analytical and bioanalytical chemistry* **2013**, DOI: 10.1007/s00216-013-7183-8.
- (28) Achten, C.; Beer, F. T.; Stader, C.; Brinkhaus, S. G. *Environmental Forensics* **2015**, DOI: 10.1080/15275922.2014.991004.
- 485 (29) Kauppila, T. J.; Kersten, H.; Benter, T. *Journal of the American Society for Mass Spectrometry* **2015**, DOI: 10.1007/s13361-015-1092-3.
- (30) Thiäner, J. B.; Achten, C. *Analytical and bioanalytical chemistry* **2017**, DOI: 10.1007/s00216-016-0121-9.
- (31) Thiäner, J. B.; Richter-Brockmann, S.; Achten, C. *Journal of chromatography. A* **2018**, DOI: 490 10.1016/j.chroma.2018.10.028.
- (32) Kauppila, T. J.; Kersten, H.; Benter, T. *Journal of the American Society for Mass Spectrometry* **2014**, DOI: 10.1007/s13361-014-0988-7.
- (33) Lorenz, M.; Schiewek, R.; Brockmann, K. J.; Schmitz, O. J.; Gäb, S.; Benter, T. *Journal of the American Society for Mass Spectrometry* **2008**, DOI: 10.1016/j.jasms.2007.11.021.
- 495 (34) Hanley, L.; Zimmermann, R. *Analytical chemistry* **2009**, DOI: 10.1021/ac8013675.
- (35) Zimmermann, R. *Analytical and bioanalytical chemistry* **2013**, DOI: 10.1007/s00216-013-7187-4.
- (36) Streibel, T.; Zimmermann, R. *Annual review of analytical chemistry (Palo Alto, Calif.)* **2014**, DOI: 10.1146/annurev-anchem-062012-092648.
- (37) Jennerwein, M. K.; Eschner, M. S.; Wilharm, T.; Zimmermann, R.; Gröger, T. M. *Energy Fuels* 500 **2017**, DOI: 10.1021/acs.energyfuels.7b01799.
- (38) Rüger, C. P.; Schwemer, T.; Sklorz, M.; O'Connor, P. B.; Barrow, M. P.; Zimmermann, R. *European Journal of Mass Spectrometry* **2017**, DOI: 10.1177/1469066717694286.
- (39) Rüger, C. P.; Neumann, A.; Sklorz, M.; Schwemer, T.; Zimmermann, R. *Energy and Fuels* **2017**, 31 (12), 13144–13158.
- 505 (40) Kuroda, H. *Nature* **1964**, DOI: 10.1038/2011214a0.
- (41) Linstrom, P. J.; Mallard, W.G. (Eds.). *NIST Chemistry WebBook*.
- (42) Gehm, C.; Streibel, T.; Passig, J.; Zimmermann, R. *Applied Sciences* **2018**, DOI: 10.3390/app8091617.
- (43) Adam, T.; Zimmermann, R. *Analytical and bioanalytical chemistry* **2007**, DOI: 10.1007/s00216-007-1571-x.
- 510 (44) Eschner, M. S.; Zimmermann, R. *Applied spectroscopy* **2011**, DOI: 10.1366/11-06233.
- (45) Mühlberger, F.; Hafner, K.; Kaesdorf, S.; Ferge, T.; Zimmermann, R. *Analytical chemistry* **2004**, DOI: 10.1021/ac049535r.
- (46) Eliasson, B.; Kogelschatz, U. *Ozone: Science & Engineering* **1991**, DOI: 515 10.1080/01919519108552472.
- (47) Keyte, I. J.; Harrison, R. M.; Lammel, G. *Chemical Society reviews* **2013**, DOI: 10.1039/C3CS60147A.
- (48) Miet, K.; Le Menach, K.; Flaud, P. M.; Budzinski, H.; Villenave, E. *Atmospheric Environment* **2009**, DOI: 10.1016/j.atmosenv.2009.04.032.
- 520 (49) Hughey, C. A.; Hendrickson, C. L.; Rodgers, R. P.; Marshall, A. G.; Qian, K. *Analytical chemistry* **2001**, DOI: 10.1021/ac010560w.

## Supporting Information

### **Atmospheric pressure single photon laser ionization (APSPLI) mass spectrometry using a 157 nm fluorine excimer laser for sensitive and selective detection of non- to semi-polar hydrocarbons**

Christopher P. Rüger<sup>1,2\*#</sup>, Anika Neumann<sup>1,2#</sup>, Martin Sklorz<sup>3</sup>, Ralf Zimmermann<sup>1,2,3</sup>

1 Joint Mass Spectrometry Centre, Chair of Analytical Chemistry, University of Rostock,  
18059 Rostock, Germany

2 Department Life, Light & Matter (LLM), University of Rostock, 18051 Rostock, Germany

3 Joint Mass Spectrometry Centre, Cooperation Group "Comprehensive Molecular Analytics"  
(CMA), Helmholtz Zentrum München (HMGU), 85764 Neuherberg, Germany

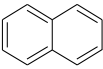
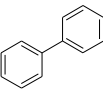
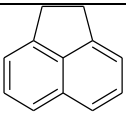
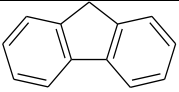
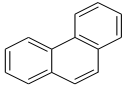
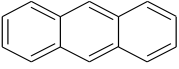
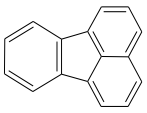
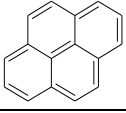
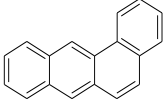
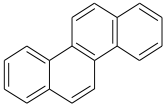
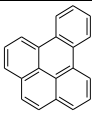
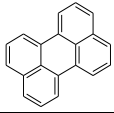
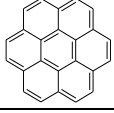
**Keywords:** atmospheric pressure laser ionization (APLI), excimer laser, high-resolution mass spectrometry, polycyclic aromatic hydrocarbons (PAH), gas chromatography

\* corresponding author, [christopher.rueger@uni-rostock.de](mailto:christopher.rueger@uni-rostock.de)

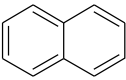
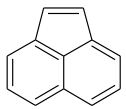
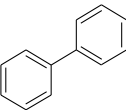
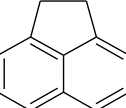
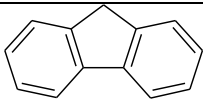
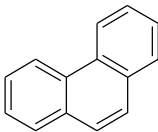
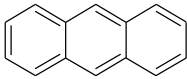
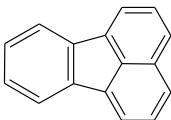
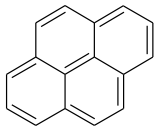
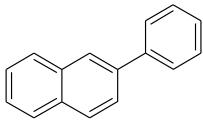
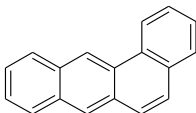
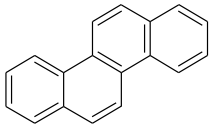
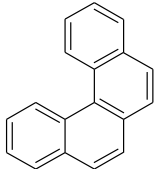
# these authors contributed equally to the manuscript

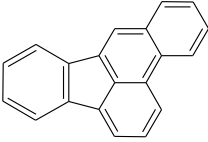
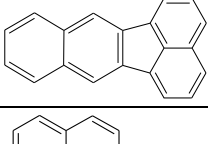
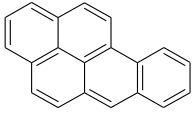
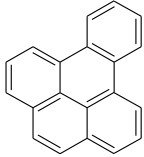
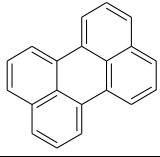
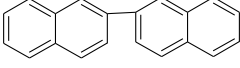
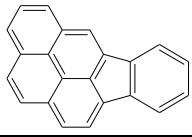
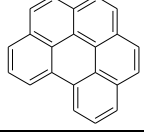
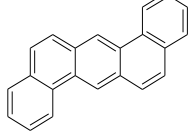
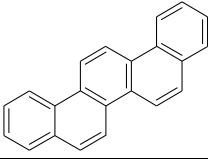
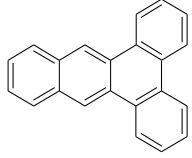
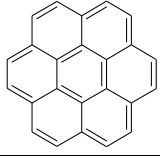
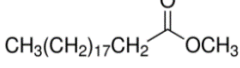


**Table S1:** Composition of the A4 polycyclic aromatic hydrocarbon standard mixture. Structure, concentration, molecular formula and exact mass are given.

#	Structure	Name, sum formula, exact mass	Concentration [mg/l]
1		Naphthalene $C_{10}H_8$ 128.062600	7.65
2		Biphenyl $C_{12}H_{10}$ 154.078250	1.95
3		Acenaphthene $C_{12}H_{10}$ 154.078250	7.96
4		Fluorene $C_{13}H_{10}$ 166.078250	9.21
5		Phenanthrene $C_{14}H_{10}$ 178.078250	8.57
6		Anthracene $C_{14}H_{10}$ 178.078250	8.08
7		Fluoranthene $C_{16}H_{10}$ 202.078250	7.72
8		Pyrene $C_{16}H_{10}$ 202.078250	9.22
9		Benz[a]anthracene $C_{18}H_{12}$ 228.093900	1.26
10		Chrysene $C_{18}H_{12}$ 228.093900	1.65
11		Benzo[e]pyrene $C_{20}H_{12}$ 252.093900	1.77
12		Perylene $C_{20}H_{12}$ 252.093900	1.48
13		Coronene $C_{24}H_{12}$ 300.093900	1.43

**Table S2:** Composition of the M3 polycyclic aromatic hydrocarbon standard mixture. Structure, concentration, molecular formula and exact mass are given.

#	Structure	Name, sum formula, exact mass	Concentration [mg/l]
1		Naphthalene $C_{10}H_8$ 128.062600	4.95
2		Acenaphthylene $C_{12}H_8$ 152.062600	4.38
3		Biphenyl $C_{12}H_{10}$ 154.078250	0.77
4		Acenaphthene $C_{12}H_{10}$ 154.078250	4.89
5		Fluorene $C_{13}H_{10}$ 166.078250	5.53
6		Phenanthrene $C_{14}H_{10}$ 178.078250	4.76
7		Anthracene $C_{14}H_{10}$ 178.078250	1.30
8		Fluoranthene $C_{16}H_{10}$ 202.078250	1.70
9		Pyrene $C_{16}H_{10}$ 202.078250	2.37
10		2-Phenylnaphthalene $C_{16}H_{12}$ 204.093900	0.76
11		Benz[a]anthracene $C_{18}H_{12}$ 228.093900	1.69
12		Chrysene $C_{18}H_{12}$ 228.093900	1.64
13		Benzo(c)phenanthrene (3,4-Benzophenanthrene) $C_{18}H_{12}$ 228.093900	0.78

14		Benzo[b]fluoranthene $C_{20}H_{12}$ 252.093900	0.60
15		Benzo[k]fluoranthene $C_{20}H_{12}$ 252.093900	0.86
16		Benzo[a]pyrene $C_{20}H_{12}$ 252.093900	0.78
17		Benzo[e]pyrene $C_{20}H_{12}$ 252.093900	0.81
18		Perylene $C_{20}H_{12}$ 252.093900	0.43
19		2,2'-Binaphthyl $C_{20}H_{14}$ 254.109550	0.77
20		Indeno[1,2,3,c,d]pyrene $C_{22}H_{12}$ 276.093900	0.41
21		Benzo[g,h,i]perylene $C_{22}H_{12}$ 276.093900	0.42
22		Dibenz[a,h]anthracene $C_{22}H_{14}$ 278.109550	0.43
23		Picene $C_{22}H_{14}$ 278.109550	0.33
24		Dibenz[a,c]anthracene (1,2,3,4-Dibenzanthracene) $C_{22}H_{14}$ 278.109550	0.74
25		Coronene $C_{24}H_{12}$ 300.093900	0.44
26		Methyl eicosanoate $CH_3(CH_2)_{18}COOCH_3$ 326.318480	0.70

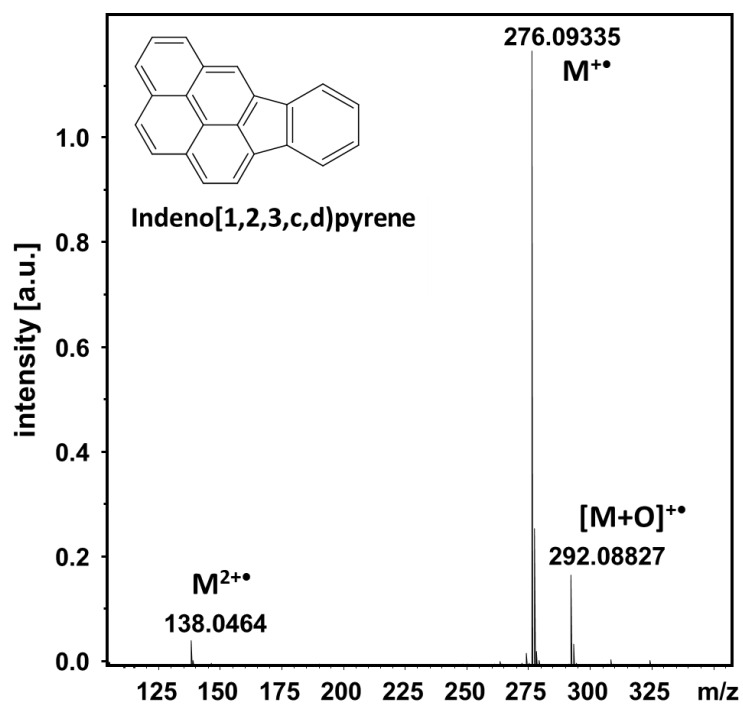


**Figure S1:** Atmospheric pressure single-photon laser ionization (APSPIL) of Indeno[1,2,3,c,d]pyrene subjected to the source by gas chromatography coupling. Aside of the characteristic oxidation ionization artifact  $[M+O]^{+•}$ , doubly charged species  $[M+O]^{2+•}$  can particularly be found for species with high aromaticity (high DBE).

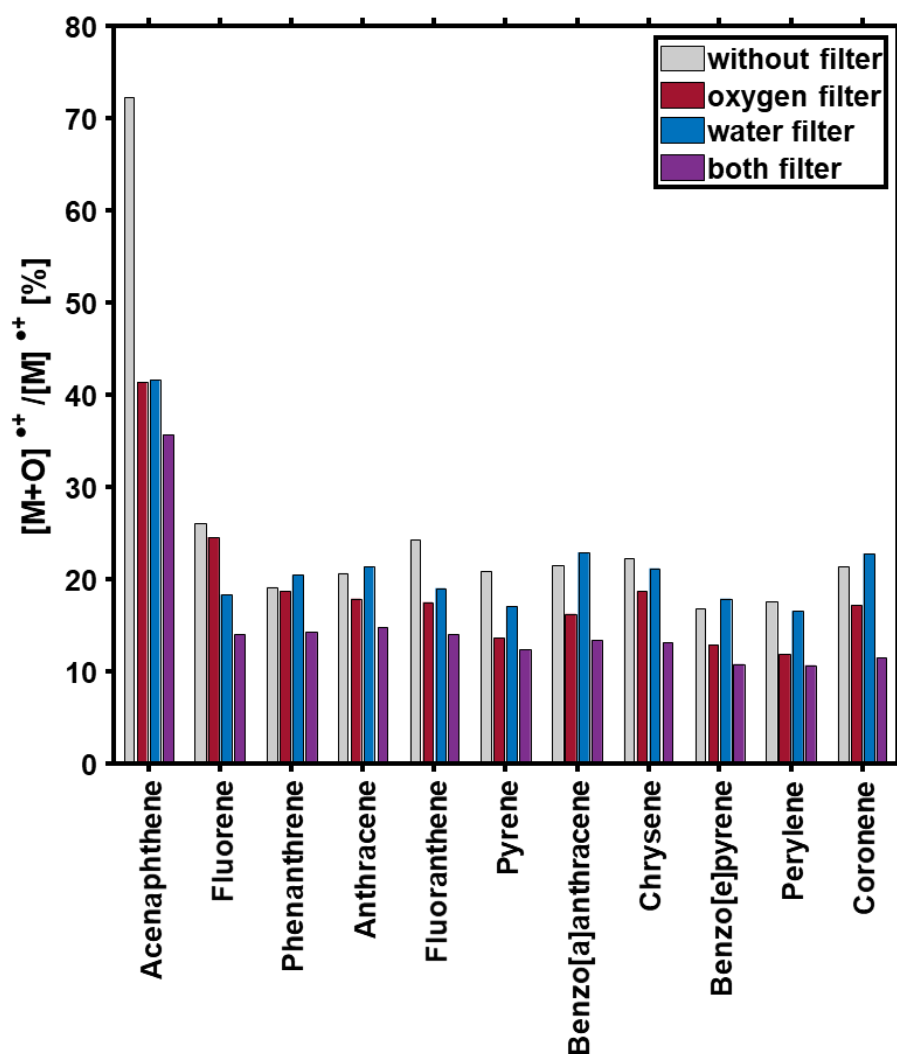


**Figure S2:** Effect of deploying an oxygen-, a water-filter, and both filter types for purification of the nebulizer gas supply to the relative occurrence of the oxidized ionization artifact  $[M+O]^{\bullet+}$  compared to the molecular radical cation  $[M]^{\bullet+}$ .

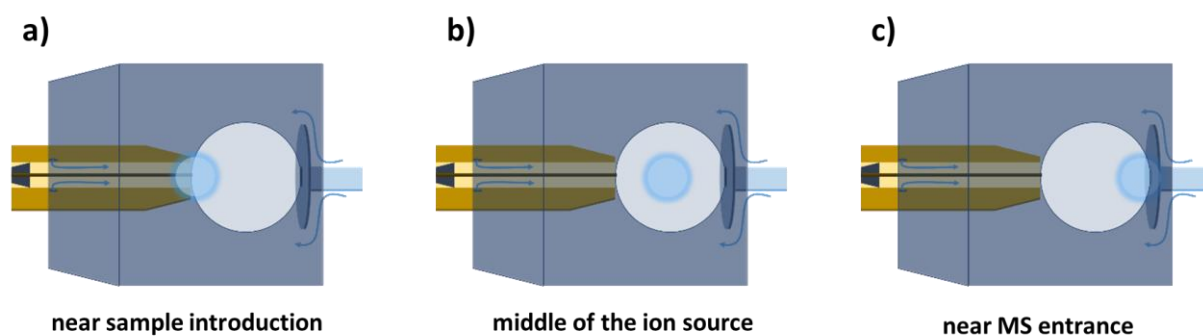


**Figure S3:** Visualizing the variation of the laser beam position (diameter  $\sim 7$  mm). Schematic cut through the ionization chamber with evolved gas analysis (EGA) exhaust at the left and mass spectrometric inlet at the right. Laser beam position a) near the sample (EGA) introduction, b) in the middle of the ion source, and c) close to the mass spectrometry entrance.

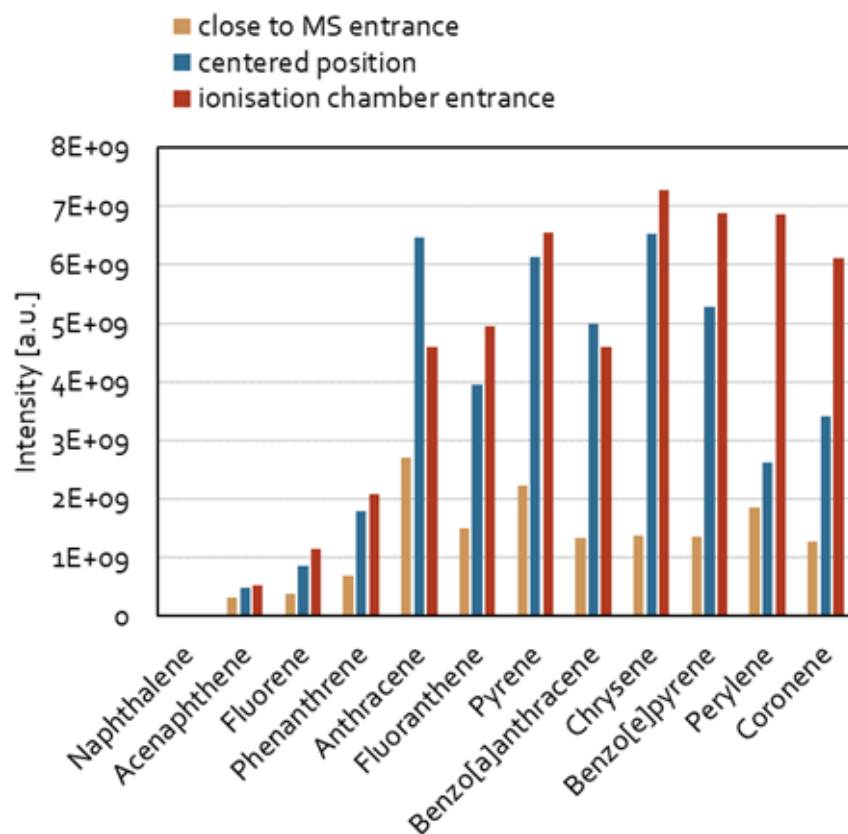


**Figure S4:** Selected compounds of the PAH standard mixture ionized by APSPLI at different positions in the ion source. The intensity of the radical cations (depicted at the ordinate) strongly depends on the ionization location.

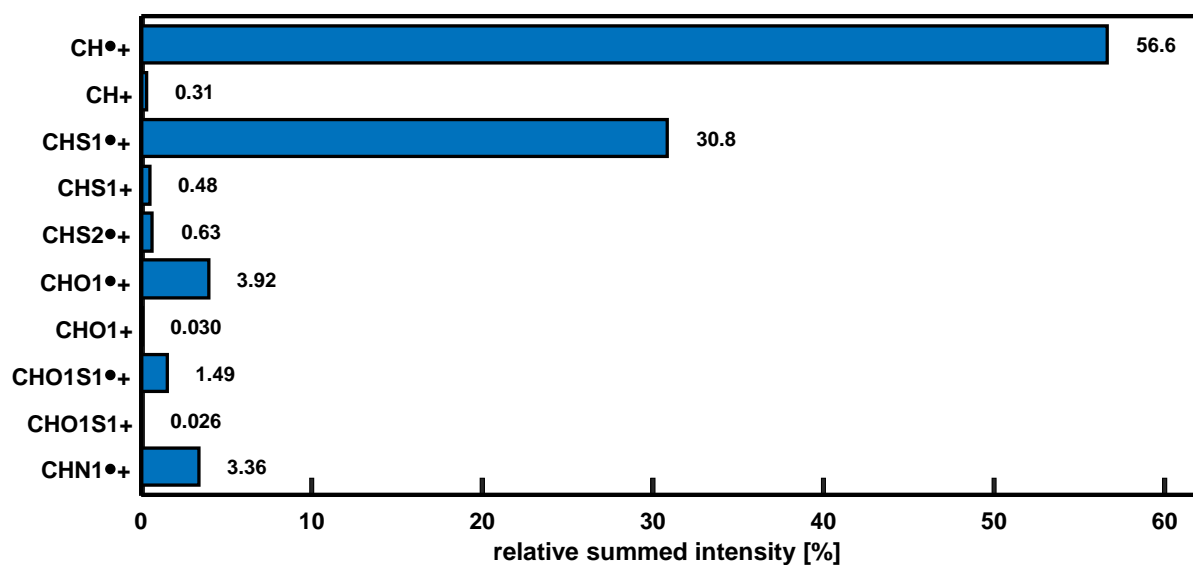


**Figure S5:** Compound class distribution of the light crude oil introduced by GC and ionized by APSPLI. The classes are divided into the respective radical cation (odd-electron configuration) and protonated species (even-electron configuration). Primarily radical cations could be found with a factor of 60-180 higher abundances compared to the protonated species.



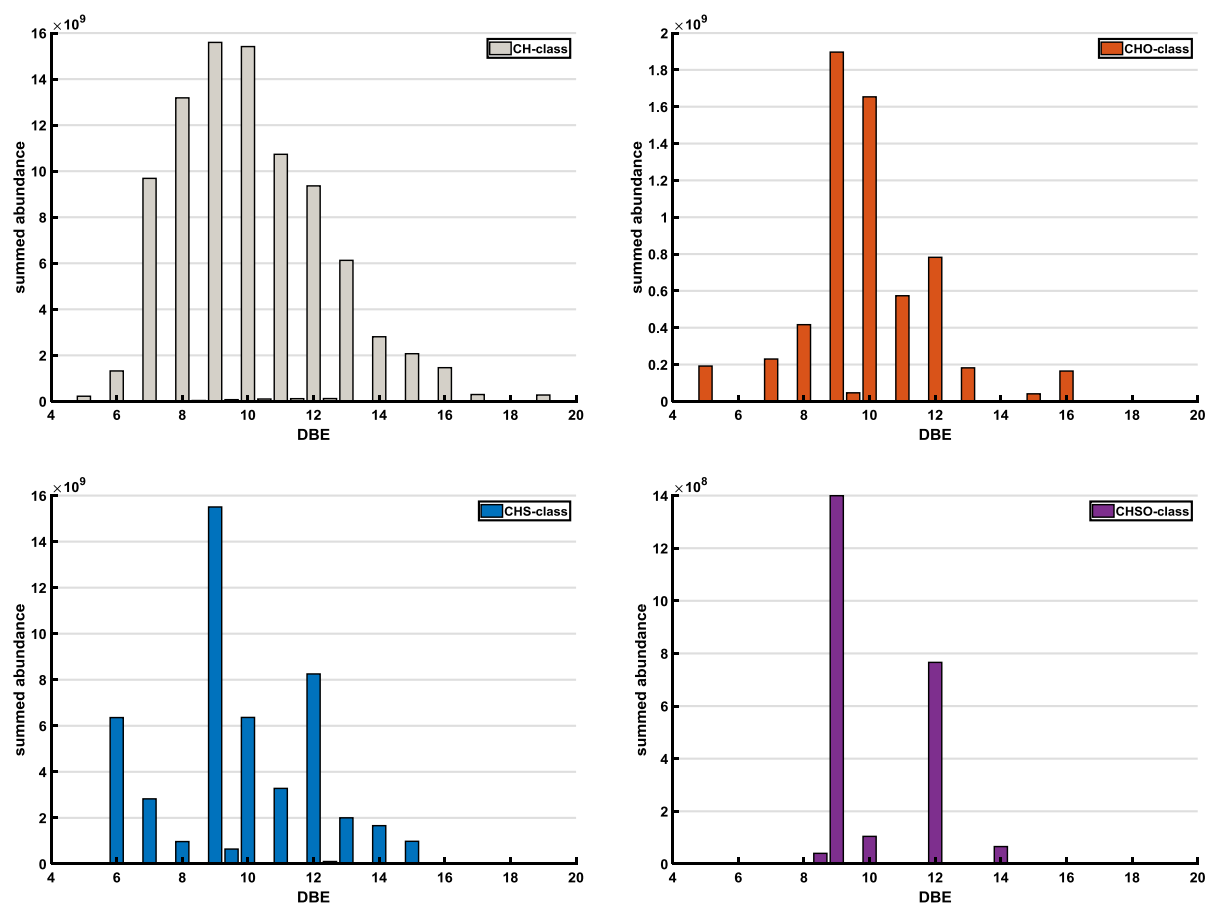


**Figure S6:** Double bond equivalent (DBE) distribution for the CH-, CHO-, CHS- and CHSO-class. The pattern between the CHO- and CH- as well as between CHS- and CHSO-class significantly differ indicating a rather low contribution of oxidized ionization artifacts.